JOURNAL OF BACTERIOLOGY, Aug. 2011, p. 4113–4122 Vol. 193, No. 16
0021-9193/11/$12.00 doi:10.1128/JB.00196-11

Alterations in the β Flap and β′ Dock Domains of the RNA Polymerase Abolish NusA-Mediated Feedback Regulation of the *metY-nusA-infB* Operon▽

Göran O. Bylund,† Stefan Nord,§ J. Mattias Lövgren,‡ and P. Mikael Wikström*

Department of Molecular Biology, Umeå University, SE-901 87 Umeå, Sweden

Received 11 February 2011/Accepted 4 June 2011

The RimM protein in *Escherichia coli* is important for the *in vivo* maturation of 30S ribosomal subunits and a Δ*rimM* mutant grows poorly due to assembly and translational defects. These deficiencies are suppressed partially by mutations that increase the synthesis of another assembly protein, RbfA, encoded by the *metY-nusA-infB* operon. Among these suppressors are mutations in *nusA* that impair the NusA-mediated negative-feedback regulation at internal intrinsic transcriptional terminators of the *metY-nusA-infB* operon. We describe here the isolation of two new mutations, one in *rpoB* and one in *rpoC* (encoding the β and β′ subunits of the RNA polymerase, respectively), that increase the synthesis of RbfA by preventing NusA from stimulating termination at the internal intrinsic transcriptional terminators of the *metY-nusA-infB* operon. The *rpoB2063* mutation changed the isoleucine in position 905 of the β flap-tip helix to a serine, while the *rpoC2064* mutation duplicated positions 415 to 416 (valine-isoleucine) at the base of the β′ dock domain. These findings support previously published *in vitro* results, which have suggested that the β flap-tip helix and β′ dock domain at either side of the RNA exit tunnel mediate the binding to NusA during transcriptional pausing and termination.

The synthesis of ribosomes in bacteria such as *Escherichia coli* is highly efficient probably because of the action of ribosome maturation proteins that are not part of the mature ribosomal subunits. One of these, the RimM protein, binds to r-protein S19 in the 30S subunits (24) and also to S19 free in solution (46) and facilitates the incorporation of S19 during *in vitro* assembly of the 30S subunits (4). Mutants lacking RimM show a 7-fold-decreased growth rate and a reduced translational efficiency, resulting from a deficiency in the maturation of the 30S subunits (6, 7). Specific alterations in r-protein S13 or an increased expression of another ribosome maturation protein, RbfA, partially suppress the slow growth and translational deficiency of a Δ*rimM102* mutant (6, 7).

RbfA is encoded by the *metY-nusA-infB* operon (Fig. 1), which contains, in the direction of transcription, the *metY* gene encoding a minor form of the initiator tRNA (19), the *rimP* gene (formerly *p15a* or *yhbC*) for the ribosome maturation protein RimP (19, 31), the *nusA* gene for the transcriptional elongation factor NusA (11, 18, 41), the *infB* gene encoding the translation initiation factor IF2 (35, 39), the *rbfA* gene (12, 43), and the *truB* gene for the tRNA Ψ55 synthase (32, 43). The *metY-nusA-infB* operon contains two promoters upstream from *metY*, P_{-1} (15) and P_1 (19, 26), and a minor promoter, P_2, located between *metY* and *rimP* (37). The cleavage by RNase III at sites between *metY* and *rimP* on the polycistronic mRNA initiates the rapid degradation of the downstream RNA (37). There are two rho-independent transcriptional terminators, T_1 (CCCCGATTTATCGGGGTTTTTT) and T_2 (GGGCTTTA GGCCCTTTTTTT), between *metY* and *rimP* (18, 37) and one, T_3 (GGGGCTAACAGCCCCTTTTT), between *infB* and *rbfA* (43).

Of 29 previously isolated suppressor mutations that increased the growth rate of the Δ*rimM102* mutant MW37, three were in *rpsM*, encoding r-protein S13 (6), and 23 were genetically linked to the *metY-infB-nusA* operon (7). At least 13 of the latter mutations increased the synthesis of RbfA: one was a duplication in which one copy of the *rbfA* gene was downstream from a promoter for the *yhbM* gene; another was an insertion of IS*2* in *infB* that created a new promoter for *rbfA*; three deleted the transcriptional terminator between *infB* and *rbfA*; and eight were in the *nusA* gene, of which at least seven resulted in a deficiency in NusA-mediated feedback regulation at the two rho-independent terminators between *metY* and *rimP* (5). We describe here the identification of the three remaining suppressor mutations and the characterization of strains harboring these mutations. The mutations were localized to *rpoB* and *rpoC*, encoding the β and β′ subunit of the RNA polymerase, respectively, and shown to increase the expression of *rbfA* by abolishing NusA-mediated negative-feedback regulation at internal transcriptional terminators of the *metY-nusA-infB* operon.

MATERIALS AND METHODS

Strains and plasmids. Strains and plasmids used are listed in Table 1. A library of mini-Tn*10*Cm insertions was constructed on the *sdr-47* (suppressor to deletion of *rimM*) containing strain PW113 by using λNK1324 as described previously

* Corresponding author. Mailing address: Department of Molecular Biology, Umeå University, SE-901 87 Umeå, Sweden. Phone: 46-90-7856754. Fax: 46-90-772630. E-mail: mikael.wikstrom@molbiol.umu.se.

† Present address: Helicure AB, Tvistevägen 48, SE-907 19 Umeå, Sweden.

§ Present address: Trehörningen 63, SE-922 66 Tavelsjö, Sweden.

‡ Present address: Department of Biochemistry and Biomedical Sciences, McMaster University, Hamilton, Ontario, Canada.

▽ Published ahead of print on 17 June 2011.

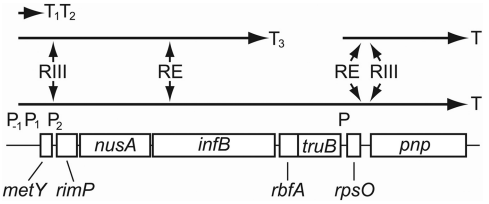

FIG. 1. Genetic organization of the *metY-nusA-infB* operon region of the chromosome. The gene *metY* encodes a minor form of the initiator tRNA, *rimP* encodes the ribosome maturation protein RimP, *nusA* encodes the transcriptional elongation factor NusA, *infB* encodes the translation initiation factor IF2; *rbfA* encodes the ribosome binding factor RbfA, *truB* encodes the tRNA Ψ55 synthase, *rpsO* encodes ribosomal protein S15, and *pnp* encodes polynucleotide phosphorylase. P_{-1}, P_1, P_2, and P indicate the locations of promoters, and T_1, T_2, T_3, and T indicate intrinsic transcriptional terminators, while RE and RIII show the cleavage sites for RNase E and RNase III, respectively. Horizontal arrows represent transcriptional products.

(22). Several clones with a mini-Tn*10*Cm linked to *sdr-47* were identified by transducing strain MW37 (Δ*rimM102*) with phage P1 grown on the library, selecting for chloramphenicol resistance (Cm^r) and screening for faster growth than that of strain MW37. One clone had a mini-Tn*10*Cm (*xxx-2423*::miniTn*10*Cm) ca. 50% linked to *sdr-47* as demonstrated by backcrosses to strain MW37 (Δ*rimM102*). From one of the backcrosses, strain GOB125 (Δ*rimM102 sdr-47 xxx-2423*::miniTn*10*Cm) was isolated and used to transfer *sdr-47* to a $rimM^+$ background by P1 transduction of the wild-type strain MW100, resulting in strain GOB250 (*sdr-47 xxx-2423*::miniTn*10*Cm) that showed a temperature-sensitive growth phenotype. To examine whether also the suppressor mutations *sdr-36* and *sdr-46* were linked to *xxx-2423*::miniTn*10*Cm, phage P1 grown on strain GOB249 ($rimM^+$ *xxx-2423*::miniTn*10*Cm), congenic to strain GOB250, was used to transduce the suppressor strains PW102 (Δ*rimM102 sdr-36*) and PW112 (Δ*rimM102 sdr-46*) selecting for Cm^r. The growth of the obtained transductants was examined by scoring the colony sizes after single-cell streaks on rich medium plates and *sdr-36* and *sdr-46*, as well as sdr^+, derivatives were obtained showing that *xxx-2423*::miniTn*10*Cm was genetically linked also to *sdr-36* and *sdr-46*. Accordingly, strains MW171 (Δ*rimM102* sdr^+ *xxx-2423*::miniTn*10*Cm), MW172 (Δ*rimM102 sdr-46 xxx-2423*::miniTn*10*Cm), and GOB307 (Δ*rimM102 sdr-36 xxx-2423*::miniTn*10*Cm) were generated. The suppressor mutations *sdr-36* and *sdr-46* were transferred from strains GOB307 and MW172, respectively, to the wild-type strain MW100 by P1 transduction and the resulting strains, MW177 (*sdr-36 xxx-2423*::miniTn*10*Cm) and MW181 (*sdr-46 xxx-2423*::miniTn*10*Cm) showed temperature-sensitive growth like the *sdr-47* containing strain GOB250 (data not shown). Strain MW176 (sdr^+ *xxx-2423*::miniTn*10*Cm) was isolated as a temperature-resistant clone from the former transduction. Both *sdr-36* and *sdr-46* were shown to be ca. 50% linked to *xxx-2423*::miniTn*10*Cm. Strains MW234 and MW237 were constructed by replacing *xxx-2423*::miniTn*10*Cm of strains MW181 and MW177, respectively, with *thi-39*::Tn*10* from CAG18500 by P1 transduction. Strains GOB896 and GOB898 were constructed by transducing strain GOB434, containing a *metY-metY*t_1t_2-*lacZ* fusion in the *lacI-lacZ* region of the chromosome, with P1 grown on strain MW234 selecting for *thi-39*::Tn*10* linked to *sdr-46* and screening for the presence of *sdr-46* or sdr^+. Strains GOB900 and GOB902 were constructed in the same way using strain MW237 as donor of *sdr-36*. Strains GOB904, GOB906, GOB908, and GOB910 were constructed in similar ways using strain GOB435, which contains a *metY-lacZ* fusion, as the recipient. Similarly, strains MW286 (*sdr-46*) and MW288 (sdr^+) are transductants of GOB838, which contains a *metY*-T_{rplS}-*lacZ* fusion, using strain MW234 as the donor, while strain MW289 (*sdr-36*) was obtained using strain MW237 as the donor.

Plasmid pMW498 expressing his_6-*nusA* from the P_{BAD} promoter was constructed in two steps. First, a DNA fragment containing the *nusA* gene was amplified by PCR using the oligonucleotides *nusA*-BamHI-F and *nusA*-HindIII-R as primers, digested with BamHI and HindIII, and ligated into BamHI/HindIII-digested His tag vector pSTN016 (31). From the resulting plasmid, pMW493, an EcoRI/HindIII fragment containing the ribosome binding site and *his6-nusA* was cloned into EcoRI/HindIII-digested pBAD30 (16).

Media and growth conditions. The minimal medium used was morpholinepropanesulfonic acid (MOPS) (30) supplemented with 0.4% glucose. Rich medium was either rich MOPS (29) or LB (2) supplemented with E+B1 (49). Cultures were grown at 37°C, and the growth was monitored either on a Zeiss PMQ3 or a Shimadzu UV-1601 spectrophotometer at 420 or 600 nm or on a Klett-Summerson colorimeter equipped with a red filter.

Localization of *xxx-2423*::miniTn*10*Cm. To localize *xxx-2423*::miniTn*10*Cm, chromosomal DNA from GOB125 (Δ*rimM102 sdr-47 xxx-2423*::miniTn*10*Cm) was digested with PstI and cloned into the low-copy-number vector pCL1921 (23), selecting for Cm^r conferred by *xxx-2423*::miniTn*10*Cm. One resulting plasmid clone, pCW2, was demonstrated by DNA sequencing with vector specific primers to contain the 90 min region of the chromosome (data not shown). The *xxx-2423*::miniTn*10*Cm had been inserted into the start codon for the *rsd* (regulator of sigma D) gene, as demonstrated by DNA sequencing out of the *xxx-2423*::miniTn*10*Cm with a primer specific for its chloramphenicol acetyltransferase gene (data not shown). Therefore, the *xxx-2423*::miniTn*10*Cm was renamed *rsd2423*::miniTn*10*Cm.

Mapping of *sdr-36*, *sdr-46*, and *sdr-47* by marker rescue. Three large overlapping subfragments of each of the *rpoB* and *rpoC* genes from the wild-type strain MW100 were generated by PCR (endpoints are listed with respect to the translational start sites)—*rpoB* (−154 to +1889, +1202 to +2845, and +2046 to +4275) and *rpoC* (−324 to +1514, +1229 to +3008, and +2653 to +4454), mainly as described by Bartlett et al. (1)—and cloned into the plasmid vector pBR322 (3). The obtained plasmids were transferred by transformation into strains MW177 (*sdr-36 rsd2423*::miniTn*10*Cm), MW181 (*sdr-46 rsd2423*::miniTn*10*Cm), and GOB250 (*sdr-47 rsd2423*::miniTn*10*Cm) selecting at 44°C to examine whether they restored growth as a result of homologous recombination between the cloned wild-type fragments and the chromosome of the temperature-sensitive *sdr* mutants.

PCR amplification of chromosomal DNA and DNA sequencing. Regions of the *E. coli* chromosome was amplified, from colonies resuspended in H_2O, by PCR (25, 40). *Pfu* DNA polymerase from Stratagene cloning systems (La Jolla, CA) was used if the obtained fragments were to be cloned into plasmids, and *Taq* DNA polymerase from Roche Diagnostics Scandinavia AB (Bromma, Sweden) was used in all other cases. Obtained fragments were separated on agarose gels, cut out, and purified by using Gene-Clean from Bio 101, Inc. (La Jolla, CA). DNA sequencing of PCR fragments was done using Thermo Sequenase, whereas plasmid DNA sequencing was performed with a T7 sequencing kit, both of which were purchased from Amersham Pharmacia Biotech (Buckinghamshire, England).

Northern blot analysis. Total RNA was prepared according to von Gabain et al. (50) and subjected to Northern blot analysis, mainly as described by Sambrook et al. (42). Equal amounts of the RNA from the different strains grown in LB medium were loaded onto the gels as determined both spectrophotometrically at 260 nm and by ethidium bromide staining of aliquots of the RNA electrophoresed in agarose gels. Probes were made with the Megaprime DNA labeling system from Amersham Pharmacia Biotech (Buckinghamshire, England) by using [α-^{32}P]dATP and DNA fragments, purified as described above, as templates.

Western blot analysis. Total cell extracts were subjected to sodium dodecyl sulfate-polyacrylamide (15%) gel electrophoresis, proteins in the gels were transferred to Hybond-ECL membranes from GE Healthcare (Uppsala, Sweden) and probed with the mouse penta-His antibody from Qiagen AB (Solna, Sweden) as recommended by the manufacturer or with an antiserum against RbfA raised in rabbit by AgriSera AB (Vännäs, Sweden). For the latter, 5% milk powder was used instead of 3% bovine serum albumin. The penta-His antibodies on the membranes were detected with a horseradish peroxidase (HRP)-conjugated rabbit anti-mouse antibody from Dako A/S, Denmark, by using an Amersham ECL Plus kit from GE Healthcare. Similarly, RbfA-antibodies were detected with an HRP-conjugated goat anti-rabbit antibody from Jackson Immunoresearch Laboratories, Inc. (West Grove, PA).

RESULTS

Three suppressor mutations to Δ*rimM102* are in *rpoB* and *rpoC*. In order to localize the three mutations *sdr-36*, *sdr-46*, and *sdr-47*, which suppress partially the slow growth of the Δ*rimM102* mutant MW37, strain GOB125 containing a mini-Tn*10*Cm linked (ca. 50%) to *sdr-47* was isolated (see Materials and Methods). The mini-Tn*10*Cm in GOB125 (Δ*rimM102 sdr-47*) was localized to the start codon of the *rsd* (regulator of sigma D) gene in the 90-min region of the chromosome (see Materials and Methods). This region of the chromosome from the sdr^+ strain GOB249 ($rimM^+$ *rsd2423*::miniTn*10*Cm) was

TABLE 1. Bacterial strains, plasmids, and oligonucleotides

Strain, plasmid, or oligonucleotide	Genotype or sequence	Source or reference[a]
Strains		
CAG18500	MG1655 *thi-39*::Tn*10*	45
GOB125	Hfr P4X Δ*rimM102 yfiB*::*nptI rpoB2063* (*sdr-47*) *rsd2423*::miniTn*10*Cm	
GOB162	Hfr P4X *rbfA*::Km^r	7
GOB249	Hfr P4X *rsd2423*::miniTn*10*Cm	
GOB250	Hfr P4X *rpoB2063* (*sdr-47*) *rsd2423*::miniTn*10*Cm	
GOB307	Hfr P4X Δ*rimM102 yfiB*::*nptI rpoC2064* (*sdr-36*) *rsd2423*::miniTn*10*Cm	
GOB434	Hfr P4X *lacI′*-T_{rplS}-P_{metY}-*metY*-*metY*-T_1T_2-*lacZ*	5
GOB435	Hfr P4X *lacI′*-T_{rplS}-P_{metY}-*metY*-*lacZ*	5
GOB750	GOB434 *nusA94 argG2424*::miniTn*10*Cm	5
GOB752	GOB435 *nusA94 argG2424*::miniTn*10*Cm	5
GOB838	Hfr P4X *lacI′*-*rplSt*-P_{metY}-*metY*-T_{rplS}-*lacZ*	5
GOB868	GOB838 *nusA94 arg2424*::miniTn*10*Cm	5
GOB896	GOB434 *rpoB2063* (*sdr-46*) *thi-39*::Tn*10*	
GOB898	GOB434 *rpoB*$^+$ *thi-39*::Tn*10*	
GOB900	GOB434 *rpoC2064* (*sdr-36*) *thi-39*::Tn*10*	
GOB902	GOB434 *rpoC*$^+$ *thi-39*::Tn*10*	
GOB904	GOB435 *rpoB2063* (*sdr-46*) *thi-39*::Tn*10*	
GOB906	GOB435 *rpoB*$^+$ *thi-39*::Tn*10*	
GOB906	GOB435 *rpoB*$^+$ *thi-39*::Tn*10*	
GOB908	GOB435 *rpoC2064* (*sdr-36*) *thi-39*::Tn*10*	
GOB910	GOB435 *rpoC*$^+$ *thi-39*::Tn*10*	
MW37	Hfr P4X Δ*rimM102 yfiB*::*nptI*	33
MW100	Hfr P4X	51
MW234	Hfr P4X *rpoB2063* (*sdr-46*) *thi-39*::Tn*10*	
MW237	Hfr P4X *rpoC2064* (*sdr-36*) *thi-39*::Tn*10*	
MW171	Hfr P4X Δ*rimM102 yfiB*::*nptI rsd2423*::miniTn*10*Cm	
MW172	Hfr P4X Δ*rimM102 yfiB*::*nptI rpoB2063* (*sdr-46*) *rsd2423*::miniTn*10*Cm	
MW176	Hfr P4X *rsd2423*::miniTn*10*Cm	
MW177	Hfr P4X *rpoC2064* (*sdr-36*) *rsd2423*::miniTn*10*Cm	
MW181	Hfr P4X *rpoB2063* (*sdr-46*) *rsd2423*::miniTn*10*Cm	
MW286	GOB838 *rpoB2063* (*sdr-46*) *thi-39*::Tn*10*	
MW288	GOB838 *rpoB*$^+$ *thi-39*::Tn*10*	
MW289	GOB838 *rpoC2064* (*sdr-36*) *thi-39*::Tn*10*	
PW102	Hfr P4X Δ*rimM102 yfiB*::*nptI sdr-36* = *rpoC2064* (Dupl. of codons 115 to 116; AGTTAT)	7
PW112	Hfr P4X Δ*rimM102 yfiB*::*nptI sdr-46* = *rpoB2063* (ATC to AGC in codon 905)	7
PW113	Hfr P4X Δ*rimM102 yfiB*::*nptI sdr-47* = *rpoB2063* (ATC to AGC in codon 905)	7
PW157	Hfr P4X Δ*rimM102 yfiB*::*nptI zhc-2421*::Tn*10*	G. O. Bylund et al.[b]
Plasmids		
pCW2	Str^r Spc^r *′rpoC yjaZ thiCEFSGH rsd2423*::miniTn*10*Cm *nudC hemE nfi yjaG hupA yjaH zraP zraS′*	
pJML007	*bla cat′ araC* P_{BAD}-*nusA*	5
pMW498	*bla cat′ araC* P_{BAD}-His_6-*nusA*	
Oligonucleotides		
nusA-BamHI-F	5′-TTTTGGATCCAACAAAGAAATTTTGGCTGTAG-3′	
nusA-HindIII-R	5′-TTTTAAGCTTTATTACGCTTCGTCACCG-3′	

[a] Unless otherwise noted, the origin was this study.
[b] G. O. Bylund, O. P. Persson, J. M. Lövgren, and P. W. Wikström, unpublished data.

able to cross out the suppressor mutations of strains PW102 (Δ*rimM102 sdr-36*) and PW112 (Δ*rimM102 sdr-46*) in P1 transduction experiments. Both *sdr-36* and *sdr-46* were ca. 50% linked to *rsd2423*::miniTn*10*Cm, indicating that they might be in the same gene as *sdr-47*. All three mutations were transferred to the wild-type strain MW100 by P1 transduction and the resulting strains, MW177 (*sdr-36 rsd2423*::miniTn*10*Cm), MW181 (*sdr-46 rsd2423*::miniTn*10*Cm), and GOB250 (*sdr-47 rsd2423*::miniTn*10*Cm) showed temperature-sensitive growth (data not shown). Since most of the previously isolated suppressor mutations to the Δ*rimM102* mutation increase the expression of the *rbfA* gene, we speculated that also the mutations *sdr-36*, *sdr-46*, and *sdr-47* might do so. Two candidate genes in this region of the chromosome for harboring mutations that could affect the expression of the *rbfA* gene were *rpoB* and *rpoC*, encoding the β and β′ subunits, respectively, of the RNA polymerase. Therefore, we tested in a marker rescue experiment whether different parts of the wild-type *rpoB* or *rpoC* genes carried on plasmids could restore the growth at 44°C of *rimM*$^+$ strains containing *sdr-36*, *sdr-46*, or *sdr-47* mutations as a result of recombination between the wild-type fragment in the plasmid and the mutant copy on the chromosome. The *rpoB* fragments +1202 to +2845 and fragments +2046 to +4275 (numbers are given with respect to the translation start site) both rescued the growth of strains MW181 (*sdr-46*) and GOB250 (*sdr-47*) at 44°C, whereas the *rpoC* frag-

ment −324 to +1514 rescued strain MW177 (*sdr-36*) (data not shown). In the region that overlapped between the two *rpoB* fragments that rescued strains MW181 (*sdr-46*) and GOB250 (*sdr-47*), there was a single mutation on the chromosome of both strains, which changed codon 905 from ATC (Ile) to AGC (Ser). The chromosomal region of strain MW177 (*sdr-36*) that corresponded to the *rpoC* fragment that rescued this strain contained a duplication of codons 415 to 416 (AGTTAT) encoding Val and Ile. These mutations will hereafter be referred to as *rpoB2063* and *rpoC2064*, respectively. In addition, the temperature sensitivity of strains containing the *rpoB2063* and *rpoC2064* mutations were complemented by plasmids pACTB1 and pACTC1, respectively, expressing wild-type copies of *rpoB* and *rpoC* (14), demonstrating that the two mutations were recessive (data not shown).

The *rpoB2063* and *rpoC2064* mutations increase the expression of the *metY-infB-nusA* operon. The growth rate in LB medium at 37°C of the original *rpoB2063* Δ*rimM102* mutants PW112 and PW113 was 2-fold higher than that of the Δ*rimM102* mutant MW37 (specific growth rates, $k = \ln 2/g$ [where g is the generation time in hours], of 0.78 and 0.39, respectively), while that of the *rpoC2064* mutant PW102 was 1.6-fold higher ($k = 0.62$). To examine whether the mechanism behind the suppression of the slow growth of the Δ*rimM102* mutant by the *rpoB2063* and *rpoC2064* mutations was an increased expression of *rbfA*, as has been seen for most of the other suppressor mutations isolated to Δ*rimM102*, the amount of RbfA in total protein extracts from Δ*rimM102*, as well as *rimM*$^+$, strains containing the *rpoB2063* or *rpoC2064* mutations was determined by Western blot analyses. Evidently, the amount of RbfA was >3-fold higher in the Δ*rimM102* mutant MW172 containing the *rpoB2063* mutation than in the congenic *rpoB*$^+$ strain MW171 (Fig. 2). The overexpression of RbfA was less in the *rpoC2064* Δ*rimM102* strain GOB307, which correlates with the slower growth of *rpoC2064* Δ*rimM102* strains compared to *rpoB2063* Δ*rimM102* strains. In a *rimM*$^+$ background, the *rpoB2063* and *rpoC2064* mutations increased the amount of RbfA approximately 6- and 5-fold, respectively (Fig. 2).

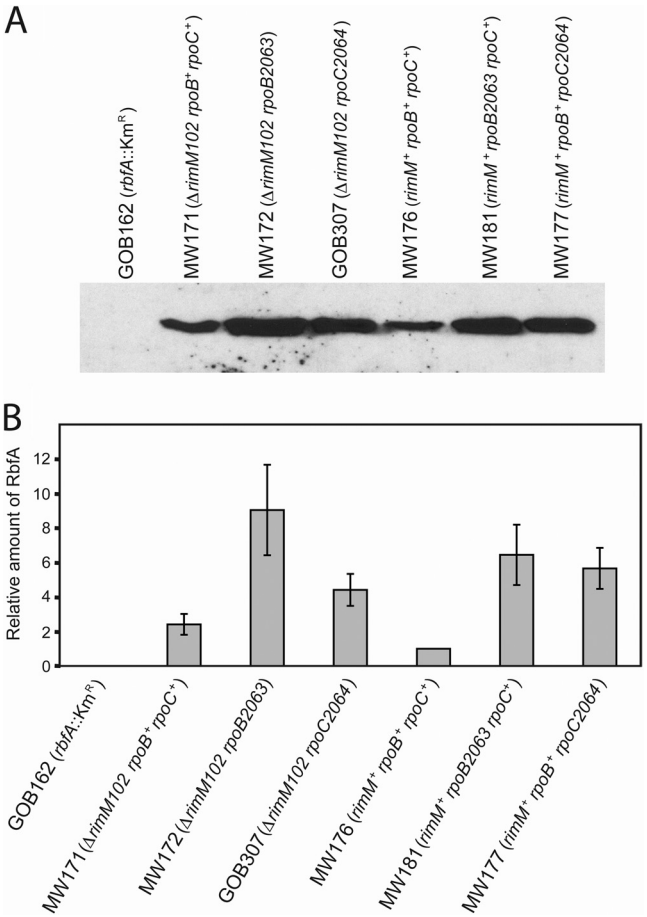

FIG. 2. Determination of the amount of RbfA in different strains. (A) Western blot analysis of cellular extracts of the indicated strains with an antiserum against RbfA. (B) Quantification of the amount of RbfA based on the results from three independent Western blot analyses. The amounts have been normalized to that obtained for the *rimM*$^+$ *rpoB*$^+$ *rpoC*$^+$ strain MW176. The standard deviation is indicated by error bars.

Conceivably, this increased amount of RbfA in strains that harbor the *rpoB2063* or *rpoC2064* mutations would result from mechanisms operating at the transcriptional level. Therefore, the effect of the two mutations on the transcriptional pattern of the *metY-nusA-infB* operon in both *rimM*$^+$ and Δ*rimM102* strains was examined by Northern blotting. The most abundant mRNA transcribed from this operon is 4.8 kb in size and results from initiation at the P_{-1} and P_1 promoters, readthrough of the two rho-independent terminators between *metY* and *rimP*, termination at the rho-independent T_3 terminator just upstream from *rbfA*, and processing by RNase III between *metY* and *rimP* (Fig. 1) (15, 19, 26, 37, 43). The production of the less-abundant 6.7-kb mRNA requires readthrough of the T_3 terminator and termination at the terminator downstream from the *pnp* gene followed by processing at the RNase III site between *rpsO* and *pnp* (36, 38, 43). Visibly, the *rpoB2063* and *rpoC2064* mutations increased the amount of both the 4.8- and the 6.7-kb mRNAs in a *rimM*$^+$ background (Fig. 3). In the Δ*rimM102* mutant, the amount of the two mRNAs was lower than in the *rimM*$^+$ background, as also has been seen previously (7). The amount of the 4.8-kb mRNA was higher in the *rpoB2063* Δ*rimM102* and *rpoC2064* Δ*rimM102* strains than in the suppressor-free Δ*rimM102* mutant. The amount of the 6.7-kb mRNA covering the *rbfA* gene was just above detection level; however, it appeared to be more abundant in the two suppressor-containing strains. This was supported by the results from a real-time reverse transcriptase PCR experiment, in which the amounts of mRNA corresponding to the *rbfA* gene were 8.6- and 2.3-fold higher in the *rpoB2063* Δ*rimM102* strain MW172 and the *rpoC2064* Δ*rimM102* strain GOB307, respectively, than in the Δ*rimM102* mutant PW157 (data not shown).

The *rpoB2063* and *rpoC2064* mutations abolish NusA-mediated feedback regulation at internal rho-independent transcriptional terminators of the *metY-nusA-infB* operon. The T_1 and T_2 rho-independent terminators between *metY* and *rimP* are a target for NusA-mediated negative-feedback regulation of the *metY-nusA-infB* operon (5, 27, 34), and different *nusA* mutations isolated as suppressors to the Δ*rimM102* mutation increase the readthrough of these terminators (5). Therefore,

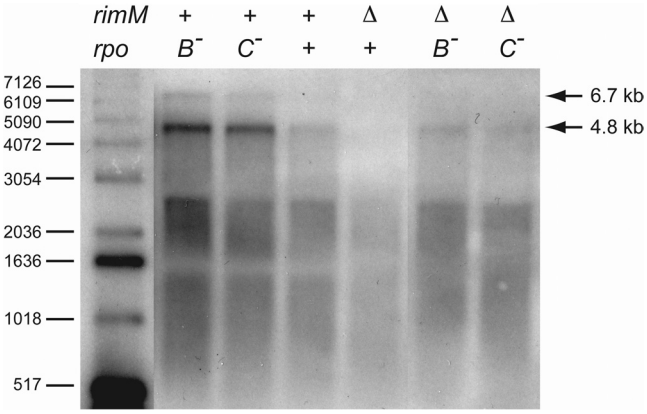

FIG. 3. Northern blot analysis of *metY-nusA-infB* operon mRNA. Portions (5 μg) of total RNA were subjected to electrophoresis in an agarose gel containing formaldehyde, transferred to a Hybond N filter, and probed with a radiolabeled DNA probe corresponding to the *rimP* gene. The sizes of the [γ-^{32}P]ATP kinase fragments of the 1-kb DNA ladder from Gibco-BRL Life Technologies, Inc. (Gaithersburg, MD), are indicated. The strains used (with relevant genetic markers in parentheses) were MW181 (*rimM*$^+$ *rpoB2063*), MW177 (*rimM*$^+$ *rpoC2064*), GOB249 (*rimM*$^+$ *rpoB*$^+$ *rpoC*$^+$), PW157 (Δ*rimM102 rpoB*$^+$ *rpoC*$^+$), MW172 (Δ*rimM102 rpoB2063*), and GOB307 (Δ*rimM102 rpoC2064*). For complete genotypes, see Table 1.

we wanted to examine whether the *rpoB2063* and *rpoC2064* mutations also increased the readthrough of these terminators. The two mutations were introduced into two strains that harbor either of two transcriptional fusions between *metY* and *lacZ*, integrated into the *lacI-lacZ* region of the chromosome. One of the fusions contains the T_1 and T_2 terminators, while the other lacks them (5). The different strains were grown at 37°C in liquid LB, supplemented with medium E+B1, and their expression of the *metY-lacZ* fusions was determined. The ratio of the β-galactosidase activity in a strain containing the fusion with the terminators to that of a strain containing the fusion that lacks the terminators, in an otherwise identical genetic background, was used as a measure of the readthrough. Interestingly, the *rpoB2063* and *rpoC2064* mutations increased readthrough approximately 1.6- and 1.2-fold, respectively (Table 2). Further, the effect of these two mutations was also tested after a shift from 37°C to the nonpermissive temperature 44°C by diluting the cultures 10-fold into prewarmed medium and assaying after two generations of growth. The temperature shift did not affect the readthrough of the terminators in any of the strains (data not shown). To examine whether the increased readthrough resulted from an inability of NusA to stimulate termination at these terminators in the two mutants, the effect of increased synthesis of NusA on the readthrough was examined. Plasmid pJML007 containing the *nusA* gene under the control of the arabinose-inducible P_{BAD} promoter was introduced into the different strains containing the *metY-lacZ* fusions. A *nusA94* mutant that shows increased readthrough of these terminators was used as a control for that the synthesis of NusA from the plasmid could restore feedback regulation (5). The *nusA94* mutant shows a temperature-sensitive growth phenotype and are unable to grow at 44°C. Therefore, the amount of arabinose to be used for achieving relevant expression of *nusA* from the plasmid was determined by testing different concentration of arabinose for the ability to support growth of the *nusA94* mutant on LA plates at 44°C. A 0.02% concentration of arabinose restored growth at 44°C of the *nusA94* strains that contained the *metY-lacZ* fusions (data not shown). Concentrations of arabinose of 0.05% and higher reduced the growth of the *nusA94* strains, as well as that of the *nusA*$^+$ strains. The growth of the *rpoB2063* and *rpoC2064* mutants, which also are unable to grow at 44°C, was not promoted by synthesis of NusA from the plasmid. The expression of the *metY-lacZ* fusions was determined by growing the different strains at 37°C in liquid LB, supplemented with medium E+B1, without or with 0.02% of arabinose, and measuring the β-galactosidase activity in cellular extracts. In the absence of arabinose, the readthrough values of the two terminators were 1.9 and 1.7 times higher in the *nusA94* and *rpoB2063* mutants, respectively, than in the *nusA*$^+$ *rpoB*$^+$ *rpoC*$^+$ strain (Table 3). In the presence of arabinose, readthrough in the *nusA*$^+$ *rpoB*$^+$ *rpoC*$^+$ strain was 2.4 times lower than in the absence of arabinose, suggesting that increased synthesis of NusA from the plasmid repressed the readthrough of the two terminators. Similarly, the addition of arabinose to the *nusA94* strains repressed the readthrough almost 3-fold. However, the presence of arabinose did not significantly reduce the readthrough of the T_1 and T_2 terminators in the *rpoB2063* and *rpoC2064* mutants. Thus, the *rpoB2063* and *rpoC2064* mutants seem deficient in NusA-mediated negative-feedback regulation at these terminators.

TABLE 2. Effect of *rpoB2063* and *rpoC2064* mutations on the readthrough of transcriptional terminators between *metY* and *rimP* [a]

Expt	*rpoB* genes			*rpoC* genes		
	Readthrough		Relative readthrough (*rpoB2063*/*rpoB*$^+$)	Readthrough		Relative readthrough (*rpoC2064*/*rpoC*$^+$)
	rpoB$^+$	*rpoB2063*		*rpoC*$^+$	*rpoC2064*	
1	0.27	0.43	1.59	0.25	0.32	1.28
2	0.31	0.55	1.77	0.30	0.35	1.17
3	0.25	0.38	1.52	0.24	0.27	1.12
4	0.28	0.38	1.36	0.25	0.29	1.16
Avg			1.56			1.18

[a] Readthrough is calculated as [(P + T)/P]. The readthrough of the *metY*-T_1T_2 terminators was determined by comparing the β-galactosidase activity of the P_{metY}-*metY*-T_1T_2-*lacZ* (P + T) and P_{metY}-*metY-lacZ* (P) fusions in four independent experiments. The strains used were GOB906 (*rpoB*$^+$ [P]), GOB898 (*rpoB*$^+$ [P + T]), GOB904 (*rpoB2063* [P]), GOB896 (*rpoB2063* [P + T]), GOB910 (*rpoC*$^+$ [P]), GOB902 (*rpoC*$^+$ [P + T]), GOB908 (*rpoC2064* [P]), and GOB900 (*rpoC2064* [P + T]). For complete genotypes, see Table 1.

TABLE 3. Effect of *rpoB2063* and *rpoC2064* on NusA-mediated transcriptional feedback regulation at the terminators between *metY* and *rimP*

Genotype	Readthrough[a]				Mean fold repression ± SD[b]
	Expt 1		Expt 2		
	−Ara	+Ara	−Ara	+Ara	
nusA$^+$ *rpoB*$^+$ *rpoC*$^+$/pJML007 (*nusA*$^+$)	0.20	0.085	0.21	0.085	2.41 ± 0.06
nusA94/pJML007 (*nusA*$^+$)	0.36	0.13	0.40	0.13	2.92 ± 0.15
rpoB2063/pJML007 (*nusA*$^+$)	0.32	0.31	0.36	0.29	1.14 ± 0.10
rpoC2064/pJML007 (*nusA*$^+$)	0.17	0.22	0.24	0.21	0.95 ± 0.18

[a] Readthrough was calculated as [(P + T)/P]. The effect of induced expression of *nusA* on the readthrough of the *metY*-T_1T_2 terminators was determined in two independent experiments by comparing the β-galactosidase activity of the P_{metY}-*metY*-T_1T_2-*lacZ* (P + T) and P_{metY}-*metY*-*lacZ* (P) fusions in strains harboring plasmid pJML007 that carries *nusA* under the control of the arabinose-inducible P_{BAD} promoter. Readthrough was determined with (+Ara) or without (−Ara) the addition of 0.02% arabinose. Only relevant genotypes are indicated. For complete genotypes. see Table 1. The strains used were GOB906/pJML007, GOB898/pJML007, GOB752/pJML007, GOB750/pJML007, GOB904/pJML007, GOB896/pJML007, GOB908/pJML007, and GOB900/pJML007.

[b] The repression was calculated as the ratio of the readthrough in the absence of arabinose to that in the presence of arabinose.

Formally, the lack of effect on the expression of β-galactosidase by the addition of arabinose to the *rpoB2063* and *rpoC2064* mutants could have resulted from the fact that NusA was not produced from plasmid pJML007 due to an inability of the mutant RNA polymerases to initiate transcription at the P_{BAD} promoter. Therefore, the ability of arabinose to induce expression from this promoter in the *rpoB2063* and *rpoC2064* mutants MW181 and MW177, as well as the *rpoB*$^+$ *rpoC*$^+$ strain MW176, was tested in a Western blotting experiment. A His_6-*nusA* construct was placed downstream from the P_{BAD} promoter in plasmid pBAD30, i.e., the same vector that pJML007 is based on, and the amount of the His_6-NusA protein in the three strains grown at 37°C in LB, without or with 0.02% arabinose, was examined using antibodies against the His tag. No detectable amount of the His_6-NusA protein was observed in the absence of arabinose, whereas in the presence of arabinose a severalfold-higher expression was seen for all three strains (Fig. 4). Thus, the P_{BAD} promoter is functional in the *rpoB2063* and *rpoC2064* mutants, suggesting that the lack of effect on the readthrough of the T_1 and T_2 terminators between *metY* and *rimP* upon addition of arabinose (Table 3) indeed resulted from an inability of NusA to support transcriptional termination at these terminators when the RNA polymerase contained either of the alterations brought about by the *rpoB2063* and *rpoC2064* mutations.

The *rpoB2063* mutation also affects transcriptional termination at the terminator of the *trmD* operon. To investigate whether the effect of the *rpoB2063* and *rpoC2064* mutations on transcriptional termination was limited to terminators of the *metY-nusA-infB* operon or if the two mutations also affected termination at other terminators, the readthrough of the rho-independent major terminator, T_{rplS}, of the *trmD* operon (which encodes ribosomal proteins S16 and L19, the ribosome maturation protein RimM, and the tRNAm^{1}G37methyltransferase) (8, 9) was studied. Previously, the readthrough of the T_{rplS} terminator was shown to be 2.2-fold higher in a *nusA94* mutant than in a *nusA*$^+$ strain when this terminator was present in the terminator-containing *metY-lacZ* fusion used above, in place of the *metY* T_1 and T_2 terminators (5). The *rpoB2063* and *rpoC2064* mutations were introduced into the *metY-lacZ* fusion strain containing the T_{rplS} terminator, and their effect on the readthrough was determined. The *rpoB2063* mutation increased the readthrough of this terminator 1.6-fold, while the *rpoC2064* mutation seemed not to affect the readthrough (Table 4). Further, the effect of increased expression of *nusA* on the readthrough of the T_{rplS} terminator was examined by introducing plasmid pJML007 (P_{BAD}-*nusA*$^+$) into the *rpoB2063* and *rpoC2064* mutants, as well as the *nusA94* mutant, and inducing the expression of *nusA*$^+$ by arabinose, as described above. The increased expression of *nusA*$^+$ in the *nusA94* mutant reduced the readthrough of the T_{rplS} terminator 1.7-fold, partially restoring termination at this terminator (Table 4). However, increased expression of *nusA*$^+$ in the *rpoB2063* mutant did not reduce but on the contrary seemed to increase the readthrough. Induced expression of *nusA*$^+$ in a *nusA*$^+$ *rpoB*$^+$ *rpoC*$^+$ genetic background did not further reduce readthrough of the T_{rplS} terminator, suggesting that termination at T_{rplS} is close to maximal at normal levels of NusA. Increased expression of *nusA*$^+$ in the *rpoC2064* mutant seemed to slightly reduce readthrough. In conclusion, the *rpoB2063* mutation not only affects transcriptional

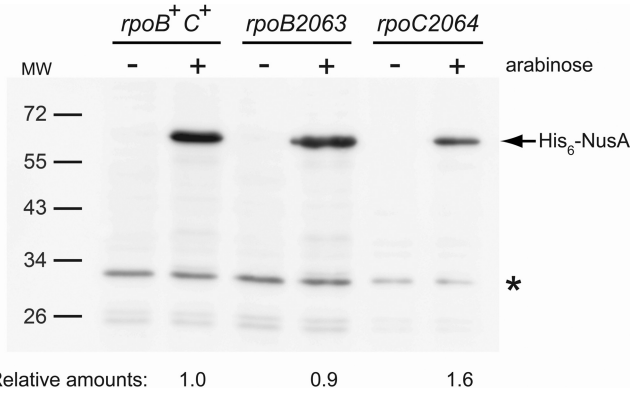

FIG. 4. Expression of His_6-*nusA* from the P_{BAD} promoter in *rpo*$^+$, *rpoB2063*, and *rpoC2064* strains as determined by Western blot analysis. Total cellular extracts of strains grown in the presence (0.02%) or absence of arabinose were probed on filters with an antibody against the His tag. The strains used (with relevant genetic markers in parentheses) were MW176/pMW498 (*rpoB*$^+$ *rpoC*$^+$/his_6-*nusA*), MW181/pMW498 (*rpoB2063 rpoC*$^+$/his_6-*nusA*), and MW177/pMW498 (*rpoB*$^+$ *rpoC2064*/his_6-*nusA*). For complete genotypes, see Table 1. MW, molecular mass marker with sizes in kilodaltons. The relative amounts of His_6-NusA shown were obtained by using an unknown protein (*) for which the synthesis did not respond to addition of arabinose as an internal control and normalizing the obtained ratios to that for the *rpoB*$^+$ *rpoC*$^+$ strain.

TABLE 4. Effect of *rpoB2063* and *rpoC2064* mutations on the readthrough of the rho-independent transcriptional terminator, T_{rplS}, of the *trmD* operon[a]

Genotype	Readthrough	Relative readthrough[b]	Genotype	Readthrough		Mean fold repression ± SD[c]
				–Ara	+Ara	
rpoB$^+$ *rpoC*$^+$	0.084	1.0	*nusA*$^+$ *rpoB*$^+$ *rpoC*$^+$/pJML007 (*nusA*$^+$)	0.090	0.099	1.00 ± 0.09
				0.090	0.083	
rpoB2063	0.13	1.55	*rpoB2063*/pJML007 (*nusA*$^+$)	0.19	0.23	0.75 ± 0.08
				0.16	0.24	
rpoC2064	0.086	1.02	*rpoC2064*/pJML007 (*nusA*$^+$)	0.098	0.083	1.19 ± 0.01
				0.12	0.10	
			nusA94/pJML007 (*nusA*$^+$)	0.21	0.11	1.66 ± 0.24
				0.17	0.12	

[a] Readthrough was calculated as [(P + T)/P]. The readthrough of the T_{rplS} terminator was determined by comparing the β-galactosidase activity of P_{metY}-*metY*-T_{rplS}-*lacZ* (P + T) and P_{metY}-*metY*-*lacZ* (P) fusions. The effect of induced expression of *nusA* on the readthrough of this terminator was studied by measuring the β-galactosidase activity in strains harboring plasmid pJML007 that carries *nusA* under the control of the arabinose-inducible P_{BAD} promoter. Readthrough was determined with (+Ara) or without (−Ara) the addition of 0.02% arabinose. Only relevant genotypes are indicated. For complete genotypes, see Table 1. The P + T strains used were MW288 (*rpoB*$^+$ *rpoC*$^+$), MW286 (*rpoB2063*), MW289 (*rpoC2064*), GOB838/pJML007 (*rpoB*$^+$ *rpoC*$^+$ *nusA*$^+$/*nusA*$^+$), MW286/pJML007 (*rpoB2063*/*nusA*$^+$), MW289/pJML007 (*rpoC2064*/*nusA*$^+$), and GOB868/pJML007 (*nusA94*/*nusA*$^+$); the P strains used were GOB906 (*rpoB*$^+$ *rpoC*$^+$), GOB904 (*rpoB2063*), GOB908 (*rpoC2064*), GOB906/pJML007 (*rpoB*$^+$ *rpoC*$^+$ *nusA*$^+$/*nusA*$^+$), GOB904/pJML007 (*rpoB2063*/*nusA*$^+$), GOB908/pJML007, (*rpoC2064*/*nusA*$^+$), and GOB752/pJML007 (*nusA94*/*nusA*$^+$).

[b] For determination of the relative readthrough, the readthrough was normalized to that obtained with *nusA*$^+$ *rpoB*$^+$ *rpoC*$^+$ strains.

[c] The mean fold repression was calculated as the ratio of the readthrough in the absence to that in the presence of arabinose (0.02%).

termination at terminators of the *metY-nusA-infB* operon but also that of the T_{rplS} terminator of the *trmD* operon.

DISCUSSION

We have identified here a mutation in each of the *rpoB* and *rpoC* genes encoding the β and β′ subunits, respectively, of the RNA polymerase. The two mutations, *rpoB2063* and *rpoC2064*, isolated as suppressors of the slow growth of a strain lacking the ribosome maturation protein RimM, were found to increase the synthesis of RbfA, another ribosome maturation protein. Most of the suppressor mutations isolated in the same screen showed increased expression of *rbfA*; however, the mechanism varied (5). Eight of the suppressor mutations lead to alterations in the transcriptional elongation factor NusA which resulted in a reduced ability of NusA to stimulate transcription termination at internal rho-independent terminators of the *metY-nusA-infB* operon, thereby increasing expression of the distally located *rbfA* (5). The *rpoB2063* and *rpoC2064* mutations characterized here seem to increase the readthrough of the terminators by the same mechanism as the *nusA* mutations.

The level of arabinose that induced sufficient expression of NusA from a plasmid to complement the temperature sensitivity of a *nusA98* mutant also reduced the readthrough of the T_1 and T_2 terminators between *metY* and *rimP* in this mutant down to the level that was seen in a plasmid-free *nusA*$^+$ background (5). Further, the reduction in the readthrough was 1.8-fold both in the *nusA98* and the *nusA*$^+$ background. These findings suggested that the amount of NusA produced from the plasmid corresponded to that found in a plasmid-free *nusA*$^+$ background. Thus, an ~2-fold increased amount of NusA reduced the readthrough of these terminators almost 2-fold. NusA has been shown to stimulate pausing of the elongating RNA polymerase *in vitro* at different pause sites at equimolar amounts of NusA and RNA polymerase, whereas a 10-fold excess of NusA relative to RNA polymerase was needed to terminate transcription at rho-independent terminators (44). Thus, the role of NusA in feedback regulation at the T_1 and T_2 terminators between *metY* and *rimP* might be primarily to enhance pausing of the elongating RNA polymerase thereby facilitating transcript release or providing time for the formation of the terminator structures. However, NusA might affect termination directly at these terminators. In a large-scale computational search for bacterial transcriptional terminators, the *rimP* leader, which contains the T_1 and T_2 terminators, was the most ubiquitous transcription attenuator found (28). The stem of the T_2 terminator was found to contain the most conserved motif of all 5′ and 3′ terminators identified, suggesting that the sequence signature was specific for the *rimP* leader. Such high sequence conservation and the lack of any visible anti-terminator structure were suggested to indicate regulation by a termination or anti-termination protein such as NusA that specifically would recognize the conserved nucleic acid motif. The role of NusA at the T_1 and T_2 terminators at which it feedback regulates its own synthesis might be different from that at other terminators where the binding of NusA might be more unspecific. Thus, NusA might directly stimulate intrinsic termination at the T_1 and T_2 terminators even at lower concentrations.

The *rpoB2063* mutation reduced significantly termination at the T_1 and T_2 terminators between *metY* and *rimP* and an increased synthesis of NusA could not restore termination, suggesting that the alteration in the β subunit abolished NusA-mediated negative-feedback regulation. The effect of the *rpoC2064* mutation on the readthrough of these two terminators was small; however, increased expression of *nusA* in the *rpoC2064* mutant did not increase termination, suggesting that NusA could not promote termination at these terminators as a result of the alteration in the β′ subunit. The previously characterized *nusA* mutations have been shown to increase the readthrough also of the rho-independent terminator between *infB* and *rbfA* (5). Similarly, the *rpoB2063* and *rpoC2064* mutations increased the readthrough of the same terminator 2- and 1.5-fold, respectively, as judged from the quantification of

the readthrough (6.7 kb) and terminated transcripts (4.8 kb) in a Northern blotting experiment (data not shown).

Previously, the *nusA94* mutation was found to increase readthrough not only of the terminators of the *metY-nusA-infB* operon but also of the rho-independent *trmD* operon terminator T_{rplS} (5). We have shown here that the *rpoB2063* mutation also increased the readthrough of T_{rplS}, indicating that *rpoB2063* might have a general effect on NusA-dependent transcriptional termination. The *rpoC2064* mutation, on the other hand, did not seem to affect the readthrough of T_{rplS}. In wild-type cells, termination at T_{rplS} was not affected by increased synthesis of NusA, while at the T_1 and T_2 terminators higher levels of NusA reduced the readthrough, probably reflecting that at the latter NusA has a role to regulate its own synthesis up or down in response to different conditions and not only to maximize termination efficiency. In the *rpoB2063* mutant, increased amounts of NusA increased the readthrough of T_{rplS}, while in the *rpoC2063* mutant it slightly decreased the readthrough. This contrasts with the lack of effect at the T_1 and T_2 terminators in the two mutants at increased levels of NusA. Thus, these dissimilarities might reflect slightly different roles of NusA at the different terminators or that the two mutant RNA polymerases interact differently with different terminators.

Three mutations in *rpoB* that increased the readthrough of rho-dependent and rho-independent terminators have been shown to be incompatible with either of two mutations in *nusA* (21), one of which is identical to *nusA98* that increased the readthrough of the two terminators between *metY* and *rimP* (5). It was suggested that an enhanced readthrough of terminators accounted for the incompatibility of the *nusA* and *rpoB* mutations (21). In an attempt to introduce either of two other *nusA* alleles, *nusA91* and *nusA94*, both of which also increase the readthrough of the two terminators between *metY* and *rimP* (5), into *rpoB2063* and *rpoC2064* mutants by P1 transduction and selecting for a tightly linked resistance marker, 10- to 20-fold-lower numbers of transductants were obtained compared to when $rpoB^+$ $rpoC^+$ strains were used as recipients (data not shown). Faster-growing clones were $nusA^+$, while slower-growing ones were unstable and shown to contain both the $nusA^+$ and the respective *nusA* mutant allele showing that they were the result of insertion of the respective *nusA* mutant allele into one of two copies of the *nusA* region in a preexisting duplication. Thus, these findings suggest that mutants containing either *nusA91* or *nusA94* combined with *rpoB2063* or *rpoC2064* are not viable, possibly because of enhanced terminator readthrough. The essentiality of NusA has been attributed to its ability to increase transcriptional pausing and hence secure a tight coupling of transcription and translation (53). Thus, ribosomes bound to mRNA would prevent the transcriptional termination factor Rho from accessing it and thereby reduce premature intragenic transcriptional termination. However, more recently NusA was found to have an essential role in supporting rho-dependent termination during silencing of horizontally transferred DNA elements such as cryptic prophages, which can be toxic for the host cell when expressed (10). The *rpoB2063* and *rpoC2064* mutants show an increased sensitivity to bicyclomycin (data not shown), an antibiotic that targets the Rho protein (54). Thus, the temperature sensitivity of different *nusA* mutants, as well as of the *rpoB2063* and *rpoC2064* mutants, might result from inefficient regulation of rho-dependent termination at the higher temperatures. Conceivably, the inability to combine the *nusA91* or *nusA94* mutations with the *rpoB2063* or *rpoC2064* mutations even at lower temperatures might be explained by additive effects on rho-dependent termination.

In its role to stimulate pausing and termination of transcription elongation, NusA interacts with the RNA polymerase at the RNA exit channel by contacting the flap tip of the β subunit (β flap-tip) and the dock domain of the β′ subunit (17, 52). The removal of the β flap-tip helix (residues 900 to 909) has been shown to abolish completely NusA enhancement of pausing *in vitro* (47). Interestingly, the *rpoB2063* mutation alters the amino acid in position 905 (I905S), which is in the center of the β flap-tip helix (Fig. 5) and just next to F906 that has been shown to cross-link both to an RNA pause hairpin loop and to NusA (47). Thus, the location of the alteration in the β subunit of the *rpoB2063* mutant suggests that the reduced termination at the internal terminators of the *metY-nusA-infB* operon stem directly from a reduced ability of the mutant RNA polymerase to interact with NusA and/or the internal terminators. The inability of increased levels of NusA to restore termination suggests that the I905S substitution has a more dramatic effect than just reducing the affinity of the β flap-tip helix for NusA. Possibly, the I905S substitution confers dramatic structural changes to the β flap-tip helix so that it can no longer bind NusA.

Recently, the amino acid in position 29 of the N-terminal domain of NusA was shown by hydroxyl radical foot-printing to be close to the β′ dock domain, residues 381 to 414 in *E. coli* (17). In addition, the most common suppressor to the G181D alteration in NusA, which was one of the alterations that showed an increased readthrough of internal terminators of the *metY-nusA-infB* operon (5), is the E402K substitution in the β′ dock domain (20). These findings suggest that NusA also interacts with the β′ dock domain. The *rpoC2064* mutation characterized here resulted in a duplication of amino acids V415 and I416, which are at the base of the β′ dock domain (Fig. 5). Conceivably, the addition of these two extra amino acid residues might alter the orientation and/or structure of the β′ dock domain which would affect its interaction with NusA. The lack of effect of increased levels of NusA on the readthrough of internal transcriptional terminators of the *metY-nusA-infB* operon in the *rpoC2064* mutant is in agreement with structural changes in the β′ dock domain preventing the binding of NusA. However, the increase in readthrough of these terminators was small in the *rpoC2064* mutant compared to that in the *rpoB2063* mutant, although termination in both mutants was equally insensitive to increased amounts of NusA. Thus, the assumed structural changes in the β′ dock domain seem to have affected termination at the internal terminators of the *metY-nusA-infB* operon to become in part NusA independent.

We have presented here the first *in vivo* results that directly support an interaction of NusA with the β flap-tip and the β′ dock domain of the RNA polymerase during transcriptional termination. It would be interesting to map genetically the interaction points between NusA and the β flap-tip by con-

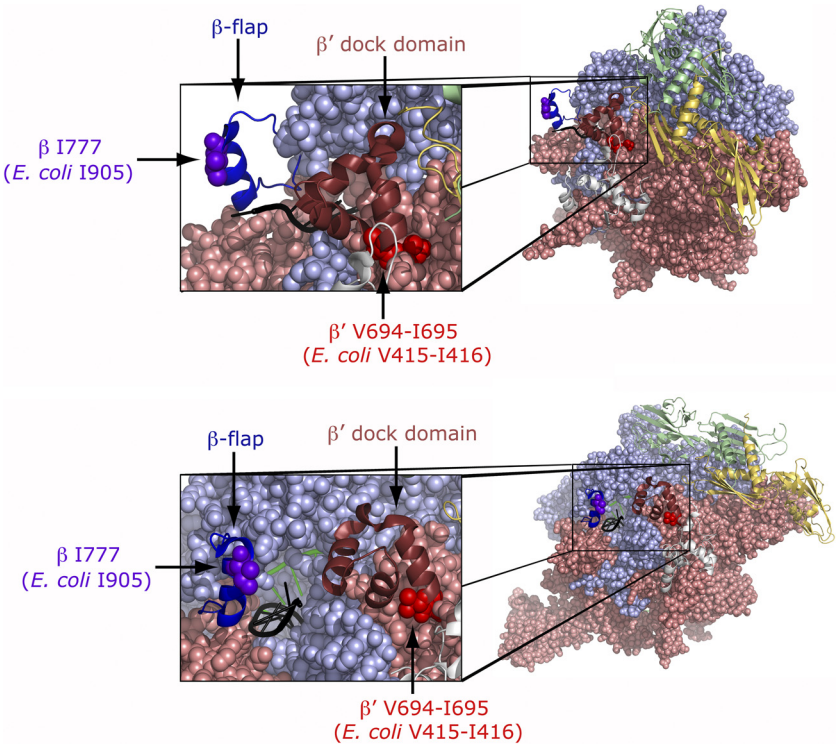

FIG. 5. Location of the amino acid alterations, conferred by the *rpoB2063* and *rpoC2064* mutations in the structure of *Thermus thermophilus* elongating complex (PDB ID, 2O5I) (48). Two different views differing by ca. 90° are shown where the two α subunits (yellow and green, respectively) and ω (light-gray) are shown as secondary-structure cartoons, while β (light-blue) and β′ (salmon) are in space-fill. In the close-ups, the β-flap domain is shown in dark blue as a cartoon with the position altered in the *rpoB2063* mutant in purple as space-fill, whereas the β′ dock domain is shown in maroon as a cartoon and at its base are the two amino acids duplicated in the *rpoC2064* mutant shown in red as space-fill. The RNA emerging from the RNA exit tunnel is in black and the DNA is in green. The structures were prepared with PyMOL (13; http://www.pymol.org).

structing mutants with conservative changes in the β flap-tip that do not destroy its structure but reduce the ability of NusA to stimulate termination at the terminators of the *metY-nusA-infB* operon and then isolate compensatory alterations in NusA expressed from a plasmid.

ACKNOWLEDGMENTS

Plasmids pACTB1 and pACTC1 were generous gifts from Derek Dykxhoorn. We thank Glenn Björk and Marcus Johansson for critical reading of the manuscript.

This research was supported by The Carl Trygger Foundation and The Magnus Bergvall Foundation.

REFERENCES

1. **Bartlett, M. S., T. Gaal, W. Ross, and R. L. Gourse.** 1998. RNA polymerase mutants that destabilize RNA polymerase-promoter complexes alter NTP-sensing by *rrn* P1 promoters. J. Mol. Biol. **279:**331–345.
2. **Bertani, G.** 1951. Studies on lysogenesis. I. The mode of phage liberation by lysogenic *Escherichia coli.* J. Bacteriol. **62:**293–300.
3. **Bolivar, F., et al.** 1977. Construction and characterization of new cloning vehicles. II. A multipurpose cloning system. Gene **2:**95–113.
4. **Bunner, A. E., S. Nord, P. M. Wikström, and J. R. Williamson.** 2010. The effect of ribosome assembly cofactors on in vitro 30S subunit reconstitution. J. Mol. Biol. **398:**1–7.
5. **Bylund, G. O., J. M. Lövgren, and P. M. Wikström.** 2001. Characterization of mutations in the *metY-nusA-infB* operon that suppress the slow-growth of a Δ*rimM* mutant. J. Bacteriol. **183:**6095–6106.
6. **Bylund, G. O., B. C. Persson, L. A. C. Lundberg, and P. M. Wikström.** 1997. A novel ribosome-associated protein is important for efficient translation in *Escherichia coli*. J. Bacteriol. **179:**4567–4574.
7. **Bylund, G. O., L. C. Wipemo, L. A. C. Lundberg, and P. M. Wikström.** 1998. RimM and RbfA are essential for efficient processing of 16S rRNA in *Escherichia coli*. J. Bacteriol. **180:**73–82.
8. **Byström, A. S., K. J. Hjalmarsson, P. M. Wikström, and G. R. Björk.** 1983. The nucleotide sequence of an *Escherichia coli* operon containing genes for the tRNA(m^1G)methyltransferase, the ribosomal proteins S16 and L19 and a 21-K polypeptide. EMBO J. **2:**899–905.
9. **Byström, A. S., A. von Gabain, and G. R. Björk.** 1989. Differentially expressed *trmD* ribosomal protein operon of *Escherichia coli* is transcribed as a single polycistronic mRNA species. J. Mol. Biol. **208:**575–586.
10. **Cardinale, C. J., et al.** 2008. Termination factor Rho and its cofactors NusA and NusG silence foreign DNA in *Escherichia coli*. Science **320:**935–938.
11. **Craven, M. G., and D. I. Friedman.** 1991. Analysis of the *Escherichia coli nusA10*(Cs) allele: relating nucleotide changes to phenotypes. J. Bacteriol. **173:**1485–1491.
12. **Dammel, C. S., and H. F. Noller.** 1995. Suppression of a cold-sensitive mutation in 16S rRNA by overexpression of a novel ribosome-binding factor, RbfA. Genes Dev. **9:**626–637.
13. **DeLano, W. L.** 2006. The PyMOL molecular graphics system, PyMOL 0.99rc6 ed. http://www.pymol.org.
14. **Dykxhoorn, D. M., R. St. Pierre, and T. Linn.** 1996. Synthesis of the β and β′ subunits of *Escherichia coli* RNA polymerase is autogenously regulated *in vivo* by both transcriptional and translational mechanisms. Mol. Microbiol. **19:**483–493.
15. **Granston, A. E., D. L. Thompson, and D. I. Friedman.** 1990. Identification of a second promoter for the *metY-nusA-infB* operon of *Escherichia coli*. J. Bacteriol. **172:**2336–2342.
16. **Guzman, L.-M., D. Belin, M. J. Carson, and J. Beckwith.** 1995. Tight regulation, modulation, and high-level expression by vectors containing the arabinose P_{BAD} promoter. J. Bacteriol. **177:**4121–4130.
17. **Ha, K. S., I. Toulokhonov, D. G. Vassylyev, and R. Landick.** 2010. The NusA N-terminal domain is necessary and sufficient for enhancement of transcriptional pausing via interaction with the RNA exit channel of RNA polymerase. J. Mol. Biol. **401:**708–725.
18. **Ishii, S., et al.** 1984. The nucleotide sequence of the cloned *nusA* gene and its flanking region of *Escherichia coli*. Nucleic Acids Res. **12:**3333–3342.
19. **Ishii, S., K. Kuroki, and F. Imamoto.** 1984. tRNAMetf2 gene in the leader region of the *nusA* operon in *Escherichia coli*. Proc. Natl. Acad. Sci. U. S. A. **81:**409–413.

20. **Ito, K., and Y. Nakamura.** 1996. Localization of *nusA*-suppressing amino acid substitutions in the conserved regions of the β′ subunit of *Escherichia coli* RNA polymerase. Mol. Gen. Genet. **251:**699–706.
21. **Jin, D. J., et al.** 1988. Effects of rifampicin resistant *rpoB* mutations on antitermination and interaction with *nusA* in *Escherichia coli*. J. Mol. Biol. **204:**247–261.
22. **Kleckner, N., J. Bender, and S. Gottesman.** 1991. Uses of transposons with emphasis on Tn*10*, p. 139–180, *Escherichia coli* and *Salmonella typhimurium*, vol. 204. Academic Press, Inc., New York, NY.
23. **Lerner, C. G., and M. Inouye.** 1990. Low copy number plasmids for regulated low-level expression of cloned genes in *Escherichia coli* with blue/white insert screening capability. Nucleic Acids Res. **18:**4631.
24. **Lövgren, J. M., et al.** 2004. The PRC-barrel domain of the ribosome maturation protein RimM mediates binding to ribosomal protein S19 in the 30S ribosomal subunits. RNA. **10:**1798–1812.
25. **Mullis, K. B., and F. A. Faloona.** 1987. Specific synthesis of DNA *in vitro* via a polymerase-catalyzed chain reaction. Methods Enzymol. **155:**335–350.
26. **Nakamura, Y., and S. Mizusawa.** 1985. In vivo evidence that the *nusA* and *infB* genes of *Escherichia coli* are part of the same multi-gene operon which encodes at least four proteins. EMBO J. **4:**527–532.
27. **Nakamura, Y., J. Plumbridge, J. Dondon, and M. Grunberg-Manago.** 1985. Evidence for autoregulation of the *nusA-infB* operon of *Escherichia coli*. Gene **36:**189–193.
28. **Naville, M., and D. Gautheret.** 2010. Premature terminator analysis sheds light on a hidden world of bacterial transcriptional attenuation. Genome Biol. **11:**R97.
29. **Neidhardt, F. C., P. L. Bloch, S. Pedersen, and S. Reeh.** 1977. Chemical measurement of steady-state levels of ten aminoacyl-tRNA synthetases in *Escherichia coli*. J. Bacteriol. **129:**378–387.
30. **Neidhardt, F. C., P. L. Bloch, and D. F. Smith.** 1974. Culture medium for enterobacteria. J. Bacteriol. **119:**736–747.
31. **Nord, S., G. O. Bylund, J. M. Lövgren, and P. M. Wikström.** 2009. The RimP protein is important for maturation of the 30S ribosomal subunit. J. Mol. Biol. **386:**742–753.
32. **Nurse, K., J. Wrzesinski, A. Bakin, B. G. Lane, and J. Ofengand.** 1995. Purification, cloning, and properties of the tRNA Ψ55 synthase from *Escherichia coli*. RNA **1:**101–112.
33. **Persson, B. C., G. O. Bylund, D. E. Berg, and P. M. Wikström.** 1995. Functional analysis of the *ffh-trmD* region of the *Escherichia coli* chromosome by using reverse genetics. J. Bacteriol. **177:**5554–5560.
34. **Plumbridge, J. A., J. Dondon, Y. Nakamura, and M. Grunberg-Manago.** 1985. Effect of NusA protein on expression of the *nusA infB* operon in *Escherichia coli*. Nucleic Acids Res. **13:**3371–3388.
35. **Plumbridge, J. A., et al.** 1982. Cloning and mapping of a gene for translational initiation factor IF2 in *Escherichia coli*. Proc. Natl. Acad. Sci. U. S. A. **79:**5033–5037.
36. **Portier, C., L. Dondon, M. Grunberg-Manago, and P. Régnier.** 1987. The first step in the functional inactivation of the *Escherichia coli* polynucleotide phosphorylase messenger is a RNase III processing at the 5′ end. EMBO J. **6:**2165–2170.
37. **Régnier, P., and M. Grunberg-Manago.** 1989. Cleavage by RNase III in the transcripts of the *metY-nusA-infB* operon of *Escherichia coli* releases the tRNA and initiates the decay of the downstream mRNA. J. Mol. Biol. **210:**293–302.
38. **Régnier, P., and C. Portier.** 1986. Initiation, attenuation and RNase III processing of transcripts from the *Escherichia coli* operon encoding ribosomal protein S15 and polynucleotide phosphorylase. J. Mol. Biol. **187:** 23–32.
39. **Sacerdot, C., P. Dessen, J. W. B. Hershey, J. A. Plumbridge, and M. Grunberg-Manago.** 1984. Sequence of the initiation factor IF2 gene: unusual protein features and homologies with elongation factors. Proc. Natl. Acad. Sci. U. S. A. **81:**7787–7791.
40. **Saiki, R. K., et al.** 1985. Enzymatic amplification of β-globin genomic sequences and restriction site analysis for diagnosis of sickle cell anemia. Science **230:**1350–1354.
41. **Saito, M., A. Tsugawa, K. Egawa, and Y. Nakamura.** 1986. Revised sequence of the *nusA* gene of *Escherichia coli* and identification of *nusA11*(Ts) and *nusA1* mutations which cause changes in a hydrophobic amino acid cluster. Mol. Gen. Genet. **205:**380–382.
42. **Sambrook, J., E. F. Fritsch, and T. Maniatis.** 1989. Molecular cloning: a laboratory manual, 2nd ed. Cold Spring Harbor Laboratory Press, Cold Spring Harbor, NY.
43. **Sands, J. F., P. Régnier, H. S. Cummings, M. Grunberg-Manago, and J. W. Hershey.** 1988. The existence of two genes between *infB* and *rpsO* in the *Escherichia coli* genome: DNA sequencing and S1 nuclease mapping. Nucleic Acids Res. **16:**10803–10816.
44. **Sigmund, C. D., and E. A. Morgan.** 1988. Nus A protein affects transcriptional pausing and termination in vitro by binding to different sites on the transcription complex. Biochemistry **27:**5622–5627.
45. **Singer, M., et al.** 1989. A collection of strains containing genetically linked alternating antibiotic resistance elements for genetic mapping of *Escherichia coli*. Microbiol. Rev. **53:**1–24.
46. **Suzuki, S., et al.** 2007. Structural characterization of the ribosome maturation protein, RimM. J. Bacteriol. **189:**6397–6406.
47. **Toulokhonov, I., I. Artsimovitch, and R. Landick.** 2001. Allosteric control of RNA polymerase by a site that contacts nascent RNA hairpins. Science **292:**730–733.
48. **Vassylyev, D. G., M. N. Vassylyeva, A. Perederina, T. H. Tahirov, and I. Artsimovitch.** 2007. Structural basis for transcription elongation by bacterial RNA polymerase. Nature **448:**157–162.
49. **Vogel, H. J., and D. M. Bonner.** 1956. Acetylornithinase of *Escherichia coli*: partial purification and some properties. J. Biol. Chem. **218:**97–106.
50. **von Gabain, A., J. G. Belasco, J. L. Schottel, A. C. Chang, and S. N. Cohen.** 1983. Decay of mRNA in *Escherichia coli*: investigation of the fate of specific segments of transcripts. Proc. Natl. Acad. Sci. U. S. A. **80:**653–657.
51. **Wikström, P. M., A. S. Byström, and G. R. Björk.** 1988. Non-autogenous control of ribosomal protein synthesis from the *trmD* operon in *Escherichia coli*. J. Mol. Biol. **203:**141–152.
52. **Yang, X., et al.** 2009. The structure of bacterial RNA polymerase in complex with the essential transcription elongation factor NusA. EMBO Rep. **10:** 997–1002.
53. **Zheng, C., and D. I. Friedman.** 1994. Reduced Rho-dependent transcription termination permits NusA-independent growth of *Escherichia coli*. Proc. Natl. Acad. Sci. U. S. A. **91:**7543–7547.
54. **Zwiefka, A., H. Kohn, and W. R. Widger.** 1993. Transcription termination factor rho: the site of bicyclomycin inhibition in *Escherichia coli*. Biochemistry **32:**3564–3570.